Possibilities of further improvement of 1-second fluxgate variometers

Andriy Marusenkov[1]

[1]Lviv Centre of Institute for Space Research, Lviv, 79060, Ukraine

Correspondence to: Andriy Marusenkov (marand@isr.lviv.ua)

Abstract. The paper discusses the possibility to improve temperature and noise characteristics of fluxgate variometers. The new fluxgate sensor with a Co-based amorphous ring core is described. This sensor is capable to improve the signal-to-noise ratio at the recording short-period geomagnetic variations. Besides the sensor performance, it is very important to create the high stability compensation field, which is cancelling the main Earth magnetic field inside the magnetic cores. For this purpose the new digitally controlled current source with low noise level and high temperature stability is developed.

1 Introduction

Flux-gate magnetometers (FGM) are widely used for measuring weak magnetic fields in geophysical researches. For this, reducing the FGM own noise is very important, particularly for observatory variometers compatible with 1-second INTERMAGNET standard (Turbitt et al., 2013). Next very important task is improving the temperature stability of both zero offset and transformation coefficient, especially for space magnetometers and geophysical equipment operating in field conditions. To reach this, the most important is to improve the FGM sensor. New approaches such as the use of ferrodielectric materials (Vetoshko et al., 2003), special excitation modes (Vetoshko et al., 2003; Koch and Rozen, 2001; Ioan et al., 2004; Sasada and Kashima, 2009; Paperno, 2004) can significantly reduce the level of own noise of flux-gate sensor, in particular, down to 0.1 pT $Hz^{-0.5}$ at a frequency of 1 Hz (Koch and Rozen, 2001) with further decrease to several tens of fT $Hz^{-0.5}$ (Koch and Rozen, 2001; Koch et al., 1999). Also in the best examples of flux-gate sensors for space research, along with moderate noise level, zero offset is practically independent on temperature: their zero drift is within 1 nT in the temperature range -40°C to +65°C (Merayo et al., 2005; Nielsen et al., 1995). In this study we try to find possibilities for simultaneous improvements of noise level and temperature stability of flux-gate variometers for Earth magnetic field measurements. In Sect. 2 we describe the new flux-gate sensor with significantly reduced noise level. Then, in Sect. 3 the peculiarities of the design of a low noise and highly stable digitally controlled current source are given.

2 Development of low-noise fluxgate sensor with amorphous magnetic core

During last fifteen - ten years our main hopes and expectations for decreasing noise level of the fluxgate sensors were linked with using amorphous magnetic materials instead of crystal permalloy for the sensor core. The very powerful technique to

suppress magnetic noise of amorphous alloy is a proper annealing procedure. The ten-fold noise level improving is possible by selection an optimal annealing temperature. However, we found also that the sensor zero offset and its temperature dependence often considerably degrade after annealing. It was experimentally found that an amorphous alloy with the lower optimal annealing temperature usually could provide lower and more stable zero offset. As a result of this approach a new amorphous ring core fluxgate sensor (conventionally named FGS32/11) had been recently developed. ~~The sensor consists of a 32 mm diameter fiberglass bobbin with 11 turns of~~ A modified version of the Co-based amorphous alloy MELTA® MM-5Co (Nosenko et al., 2008) with the Curie temperature $T_C = 185$°C and saturation induction $B_s = 0.48$ T was used as a magnetic core. The samples of this alloy were supplied by the manufacturer in the shape of 0.03 mm thick and 3 mm wide tape annealed at the temperature 710 K ~~. Besides the excitation winding it contains the two sectoral measuring winding for sensing two~~ in the atmosphere of an inert gas. The 11 turns of this tape are spooled into the 32 mm diameter fiberglass bobbin that also serves as a support for the toroidally wound measuring and excitation coils (Fig. 1, a). The four sectoral coils, the opposite pairs of which are connected in series, form the two measuring windings for sensing orthogonal components of the magnetic field (Fig. 1, b). Such unusual construction of the measuring windings was selected mainly because we found experimentally that (for this kind of magnetic cores) it provides slightly better noise level in comparison with a traditional wrapping coil. The excitation winding consists of the two layers of 0.4 mm Cu wire and has small resistance, what is preferable for minimizing drive power consumption. The sensor noise level was tested at ~~the following excitation parameters : driving frequency $f_{ex} = 7.5$~~different combination of the excitation parameters in the following ranges: the drive frequency $f_{ex} = 5 \ldots 12.5$ kHz, the amplitude of the ~~driving pulses $H_m = 6.8$~~drive pulses $H_m = 2 \ldots 10$ kA m^{-1}, and the relative width of these pulses $\alpha_{ex} = 0.2 \ldots 0.5$. The minimal noise level was achieved with $H_m = 10$ kA m^{-1} and $\alpha_{ex} = 0.5$ at the expense of considerable power consumption $P_{ex} \approx 3$ W. The compromise values $H_m = 6.8$ kA m^{-1} and $\alpha_{ex} = 0.4$ ~~.~~were finally selected. As there was no pronounced noise level dependence on the driving frequency, the intermediate value $f_{ex} = 7.5$ kHz was selected, that gives us possibility to drive two sensors simultaneously from a generator with a moderate output voltage $U_g = \pm 14$ V.

The zero offset stability and the noise level measurements were conducted in a 4-layer magnetic shield. The zero offset short-term drift lies within 40 pT during 7 hours. The sensor noise level estimations are given in Fig. 2, where for comparison purposes noise spectral density of the 1-second INTERMAGNET magnetometer LEMI-025 as well as typical geomagnetic spectrum are presented. The achieved noise level ($\leq$1 pT Hz^{-1} at 1 Hz) is three times less than that of LEMI-025, what could provide better signal-to-noise ratio especially at measurements of short-period geomagnetic variations. The zero offset ~~variations~~drift, also measured in the magnetic chamber, ~~do~~ does not exceed $\pm$1 nT during sensor temperature excursions in the range +5°C to +35°C, what is comparable with the best permalloy sensors. Due to the excellent noise level, low zero offset short-term drift and good temperature stability, this sensor is very promising for using in 1-second INTERMAGNET variometers.

~~Besides~~ During our tests of the described sensor in small fields (inside the magnetic shield or installing its sensitivity axis perpendicularly to the Earth magnetic field vector) we used the sectoral measuring windings as feedback ones. However, this way is not applicable for large magnetic field measurements, because in such case the compensation field would be considerably non-uniform and, probably, unstable with temperature and time. In order to solve this problem we are going to use these sensors

as zero field indicators inside the vector compensation coil system similar to those used in space-born magnetometers (Auster et al., 2009; Nielsen et al., 1995). So, besides the sensor performance, it is very important to create the high stability compensation field, which is canceling the main Earth magnetic field inside the magnetic cores. The possibility of constructing a digitally controlled current source (DCCS) with temperature and noise characteristics consistent with the parameters of the best modern fluxgate sensors are considered in the next section.

3 Development of digitally controlled current source

For the postulated goal achievement, following noise characteristics of the compensation field were posed: noise level no more than 0.5; 1.5 and 5 pT $Hz^{-0.5}$ at frequencies of 1; 0.1 and 0.01 Hz, respectively, what constitutes 7.1; 22 and 71 10^{-9} $Hz^{-0.5}$ in relative units taking account the compensation range of $\pm$70000 nT. Instability of compensation field should not exceed 1 nT or 14 ppm in relative units in the temperature range -40°C...+60°C. At the condition of a linear dependence of compensation field on the temperature, the thermal drift should be as small as $\leq$0.14 ppm $°C^{-1}$. The digitally controlled current source, which consists of a voltage reference (VR), a digital-to-analog converter (DAC) and ~~current-to-voltage~~ voltage-to-current converter, is analyzed.

Analysis of the literature reveals that the problem of creating a stable electric current is associated with relatively high noise level of semiconductor voltage sources. Ciofi et al. (1997) showed that radical noise reduction can be achieved using chemical current source; in the paper (Scandurra et al., 2014) reference voltage noise reduction was achieved using a low-pass filter that is based on supercapacitors. The current sources' noise characteristics achieved in (Ciofi et al., 1997; Scandurra et al., 2014) meet the requirements to the DCCS (Table 1). Table 1 also shows that the noise of the current source (Costa et al., 2012), which is built using semiconductor voltage reference, several times exceed specified limits. Devices that developed by Ciofi et al. (1997); Scandurra et al. (2014), are designed to work in the laboratory in a relatively narrow temperature range. The stability of these current sources under the temperature, time and other factors of influence is not given, but we can assume that, for example, voltage of galvanic elements and supercapacitor parameters could significantly depend on the temperature and mechanical stress.

3.1 Voltage reference selection

Basing on the detailed review of the characteristics of semiconductor integrated voltage references (Harrison, 2009) it was found that only very few models have their own noise level, temperature and time drift acceptable to be used in high-class FGM. The low-frequency ($\leq$1 Hz) noise level characteristics of different voltage reference models are given in Table 2, which is mainly filled with data taken from (Fleddermann et al., 2009; Halloin et al., 2014). Due to lack of the experimental data on the low frequency noise spectral density, we did not include in the table the first buried-zener voltage reference LM199 designed by Robert Dobkin. This IC part was used by Acuna et al. (1978) in the outstanding MAGSAT magnetometer, which performance characteristics are still impressive. An indisputable leader within all specified parameters (that was also designed by Robert Dobkin) is the buried-zener voltage reference LTZ1000 (Harrison, 2009, p. 494) based on the subsurface Zener diode, which

positive temperature coefficient is compensated by the negative coefficient of the forward-biased base-emitter voltage of the transistor located at the same substrate. This ~~voltage reference~~ product of Linear Technology (now part of Analog Devices) has also fairly weak dependence of the output voltage on the dose of radiation (Rax et al., 1997), which may be important for space application. Achieving a record low temperature drift (0.05 ppm $^{\circ}C^{-1}$) is due to crystal controlled heating and maintaining its operation temperature in a very narrow range. Taking into account the significant power consumption, this way is not always acceptable in FGM and may be unreasonable due to thermal instability of other units of the VR.

Experimental research of three samples of VR showed significant nonlinearity of the temperature dependence of the output voltage U_{REF} in the temperature compensation mode without temperature stabilization (Fig. 3), especially at the edges of the temperature range. According to Tsividis (1980) and computer modeling of the VR circuit (Fig. 4, $r_b = 0$ Ohm, $R2 =$ 18.6 Ohm, $R3 = 120$ Ohm, $R4 = 68.1$ kOhm, $R5$ is absent), conducted in LTSpiceIV simulation package, expected nonlinearity of the temperature dependence of U_{be}(VT1) and, accordingly, U_{REF} looks like a dotted curve in Fig. 3, what does not match with the measurement results of output voltage of LTZ1000 samples. Much better matching of the model curve (solid line in Fig. 3) with experiment results was obtained by adding the resistor $r_b = 15$ kOhm (Fig. 4) to the LTZ1000 circuit given in the technical documentation (Linear Technology Corp., 2015).

The U_{REF} voltage increase at low temperatures is perhaps due to a decrease of current transfer coefficient of the transistor VT1 and a corresponding increase in base current and voltage drop at r_b, $R2$ and dynamic resistance of the Zener diode VZ1, since a collector current depends slightly on the temperature (≈0.03 %/°C). To compensate the effect of the temperature dependence of the base current, and slightly linearize temperature dependence of U_{be}(VT1) is possible if to generate in the VT1 collector a current I_C proportional to absolute temperature (PTAT) of the crystal. This method is widely used for temperature compensation in bandgap voltage references (Harrison, 2009, sect. 14.1). In contrast to bandgap circuits we propose to use a simpler schematics at the expense of less accurate proportionality of the current to absolute temperature. Approximately PTAT current I_C(VT1) could be generated in the diagram in Fig. 4 at a proper value of the resistor $R5$. The result of the simulation of the modified circuit (Fig. 4 and $r_b = 15$ kOhm, $R2 = 14.5$ Ohm, $R3 = 120$ Ohm, $R4 = 30.1$ kOhm, $R5 = 6.2$ kOhm) is represented by dashed line in Fig. 3. Experimental study of the LTZ1000 sample #3, operating according to the modified circuit, showed that the output voltage U_{REF} temperature dependence becomes more linear in the temperature range from 25°C to 65°C (Fig. 5). Further it is planned to get temperature characteristics of the modified circuit in a wider temperature range, and specify parameters of the LTZ1000 to obtain more reliable results of computer simulation.

3.2 DAC configuration - bipolar vs. unipolar reference input

As a digital-to-analog converter, one of the best monolithic models – 20 bit DAC AD5791 with temperature drift 0.05 ppm $^{\circ}C^{-1}$ – was selected (Egan, 2010). As the data sheet of this component (Analog Devices, Inc., 2013) contains incomplete information regarding the noise level at low frequencies, these characteristics were examined in two circuit configurations: with bipolar (Fig. 6, Circuit 1) and unipolar (Fig. 6, Circuit 2) voltage reference input. The noise tests were carried out using the two samples of the DCCS: the sample #1 with AD5791 configured for the bipolar reference input; the sample #2 – for unipolar reference input. The voltage references were built using LTZ1000. In case of the bipolar input DAC configuration (Fig. 6, Circuit 1) the

negative reference output U_{REFN} was formed from the LTZ1000 positive output voltage U_{REFP} by a voltage inverter based on a low-noise operational amplifier AD8675 (Analog Devices, Inc., 2012) and a matched pair of the metal foil resistors DSMZ (Vishay Precision Group, Inc., 2015). The noise levels of both unipolar and bipolar voltage references were estimated before the DAC tests. It was found that the voltage inverter contributed practically no additional noise, so for both voltage references the noise level mainly depends on the LTZ1000 characteristics and are equal to $9 \cdot 10^{-9}$ Hz$^{-0.5}$ at 1 Hz; $22 \cdot 10^{-9}$ Hz$^{-0.5}$ at 0.1 Hz and $70 \cdot 10^{-9}$ Hz$^{-0.5}$ at 0.01 Hz. In each case, the DAC output was connected to the voltage-to-current converter with ungrounded load consisting of a low-noise zero-drift operational amplifier OPA2188 (Texas Instruments Inc., 2016) and high stability metal foil resistors VSMP0805 (Vishay Precision Group, Inc., 2016). The noise level of these identical voltage-to-current converters was checked separately and it did not exceed $4 \cdot 10^{-9}$ Hz$^{-0.5}$ in the frequency band $0.01 \ldots 1$ Hz. For each sample, Table 3 shows the noise level of output currents at the various points in the range: at zero ("$I_{out} = 0$" column), at the minimum ("$I_{out} = I_{min}$" column) and at the maximum values ("$I_{out} = I_{max}$" column). The values of the noise level, which exceed given limits, are marked in bold. Overpassing the requirements at a frequency of 1 Hz for both cases is caused by the voltage reference noise. The noise of the AD5791 configured with an unipolar reference input (Fig. 6, Circuit 2) is considerably bigger than that of the version with a bipolar reference input and exceeds the requirements at zero and minimum values of the output current. Probably, this is due to the additional $1/f$ noise generated by the resistors R_1, R_{FB} (see Fig. 6, Circuit 2) when a larger current is flowing through them. At the bipolar input configuration (Fig. 6, Circuit 1) these resistors are excluded from the signal pass and can not contribute an excessive noise. So, for better noise characteristics achievement, the AD5791 has to be connected in the version of the bipolar voltage reference input.

3.3 The temperature stability of the DCCS

The two prototypes of the DCCS with AD5791 configured for a bipolar reference input were intensively tested in order to estimate the temperature dependences of both the separate units and the device in whole. The measurements were carried out at the five values of the DAC input code: 0x100000 ($U_{DAC} = U_{REFN}$), 0x13FFFF ($U_{DAC} = 0.5 U_{REFN}$), 0x17FFFF ($U_{DAC} = 0$ V), 0x1BFFFF ($U_{DAC} = 0.5 U_{REFP}$) and 0x1FFFFF ($U_{DAC} = U_{REFP}$).

Let the DAC output voltage be given by expression

$$U_{DAC} = U_{REFP} S_{DAC} + U_{REFN}(1 - S_{DAC}), \tag{1}$$

where $S_{DAC} = 0 \ldots 1$ – transformation factor of the DAC.

It could be shown, that the relative deviation δS_{inv} of the voltage inverter scale factor S_{inv} leads to inconsistency of the positive U_{REFP} and negative U_{REFN} reference voltages and causes the relative change of the DAC output voltage as follows:

$$\delta U_{DAC} = \frac{\Delta U_{DAC}}{U_{REFP}} = -(1 - S_{DAC}) \delta S_{inv} \tag{2}$$

From other side the DAC output voltage could change due to the drift of the reference voltage U_{REFP} and imperfection of the internal components of the AD5791. In order to estimate full-scale and zero-scale error temperature coefficients of the AD5791 we measured simultaneously U_{REFP}, $(U_{REFP} + U_{REFN})$ and U_{DAC} during the temperature tests and applied

necessary corrections during post-processing. For instance, we estimated AD5791 zero-scale error temperature coefficient measuring $(U_{REFP} + U_{REFN})$ and $U_{DAC}(0)$ at at the nominal zero DAC output (input code 0x17FFFF, $S_{DAC} = 0.5$). Then we calculated

$$\delta U_{DAC} = \frac{\Delta U_{DAC}}{U_{REFP}}, \tag{3}$$

$$\delta S_{inv} = -\frac{(U_{REFP} + U_{REFN})}{U_{REFP}} \tag{4}$$

and analyzing sum $(\delta U_{DAC}(0) + 0.5\delta S_{inv})$ found zero-scale error temperature coefficient of the AD5791. The results of such measurements for the DCCS #1 are given in Fig. 7. The total temperature drift of the DAC output voltage $\delta U_{DAC}(0)$ (markers "$\Diamond$" in Fig. 7) is mainly caused by instability of the voltage reference inverter (markers "$\square$" in Fig. 7) and contribution of the AD5791 zero-scale error temperature drift (markers "$\circ$" in Fig. 7) is negligible. For both samples of the DCCS the AD5791 zero-scale error temperature coefficient did not exceed 0.03 ppm$^{\circ}$C^{-1} at the worst case, what is approximately compatible with data sheet specifications (Analog Devices, Inc., 2013). In both prototypes the drift of the voltage inverters' scale factors S_{inv} linearly depends on temperature with coefficients 0.27 ppm$^{\circ}$C^{-1} in the prototype #1 and 0.45 ppm$^{\circ}$C^{-1} in the prototype #2. These values coincide well with 0.5 ppm$^{\circ}$C^{-1} maximum temperature coefficient of the resistors ratio (Vishay Precision Group, Inc., 2015). The full-scale temperature coefficients of the both AD5791 did not exceed 15 ppm in the temperature range from -40°C to +60°C.

The voltage-to-current converter transforms the DAC output voltage $U_{DAC} = -7.2 \cdots + 7.2$ V into the output current $I_{out} = -3.6 \ldots + 3.6$ mA. As expected, the main contribution to the temperature drift of the transformation factor S_{ui} comes from the resistor R_{ui}, which was combined from the three surface mount resistors VSMP0805 680 Ohm connected in series. The temperature tests of the voltage-to-current converter in the DCCS #1 are given in Fig. 8. The temperature drift of the converter zero-offset (at $U_{DAC} = 0$ V, markers "$\circ$" in Fig. 8) does not exceed 5 ppm in the temperature range from -60°C to +80°C and is negligible in comparison with the temperature drift of the transformation factor. The similar results were obtained for the converter in the DCCS #2, but the transformation factor temperature dependence was much more non-linear. The temperature tests of the resistors, conducted without removing them from the boards, had confirmed that R_{ui1} and R_{ui2} depend on temperature in different ways (Fig. 9) and temperature characteristics of R_{ui2} is not compatible with data sheet specifications (Vishay Precision Group, Inc., 2016) . Probably, the reason of the R_{ui2} unexpected temperature dependence was a mechanical strain occurred, when the resistors were soldered at the board. The repeat temperature tests of the same resistors re-soldered in order to minimize possible package deformation reveal considerable change of the resistance temperature characteristic (see Fig. 9), which become more linear and similar to the data sheet curve.

4 Conclusions

The ways to improve noise level and temperature stability of 1-second fluxgate variometers are considered. The noise parameters of the new fluxgate sensor with Co-based amorphous magnetic alloy are discussed. The achieved sensor noise level is

equal to 1 pT $Hz^{-0.5}$ at 1 Hz, what is considerably better than that of the modern observatory fluxgate magnetometers. The short-term zero offset stability of the sensor is also quite good and lies within 40 pT during 7 hours. The zero offset changes do not exceed ± 1 nT during temperature excursions in the range +5°C to +35°C. Besides the sensor performance, it is very important to create the high stability compensation field, which is canceling the main Earth magnetic field inside the magnetic cores. The voltage reference in the electronic unit and the compensation windings in the sensor are the most critical elements in terms of generating the stable compensation signals. The noise level, the temperature drift, the long-term stability of the best semiconductor voltage references are compared and it is stated that only few of them are suitable for applying in high class fluxgate variometers. Using the best available electronic components the prototypes of the digitally controlled highly stable current source is designed and tested. As a part of this work it is experimentally showed, that one of the best voltage references LTZ1000 exhibits considerable non-linearity of the temperature dependence in the uncontrolled temperature mode. The curvature-compensating circuitry is proposed. The source of the extra noise in the digital-to-analog converter AD5791 is revealed and the appropriate configuration of its inner structure is selected. It is supposed that the application of the discussed in the paper results and recommendations will allow creating an FGM with outstanding level of noise and temperature parameters.

Acknowledgements. This work was supported by the grant of the National Academy of Science of Ukraine. The author would like to thank the Local Organizing Committee of XVIIth IAGA Workshop on Geomagnetic Observatory Instruments, Data Acquisition and Processing for financial support.

References

Acuna, M. H., Scearce, C. S., Seek, J., and Scheifele, J.: The MAGSAT vector magnetometer: A precision fluxgate magnetometer for the measurement of the geomagnetic field, Technical Memorandum NASA-TM-79656, National Aeronautics and Space Administration, Goddard Space Flight Center, Greenbelt, Maryland, https://ia800302.us.archive.org/34/items/nasa_techdoc_19790010349/19790010349.pdf, 1978.

Analog Devices, Inc.: 36 V Precision, 2.8 nV/$\sqrt{}$Hz Rail-to-Rail Output Op Amp. Rev. E., http://www.analog.com/media/en/technical-documentation/data-sheets/AD8675.pdf, 2012.

Analog Devices, Inc.: 1 ppm 20-Bit, ±1 LSB INL, Voltage Output DAC AD5791. Rev. D., http://www.analog.com/media/en/technical-documentation/data-sheets/AD5791.pdf, 2013.

Auster, H. U., Glassmeier, K. H., Magnes, W., Aydogar, O., Baumjohann, W., Constantinescu, D., Fischer, D., Fornacon, K. H., Georgescu, E., Harvey, P., and others: The THEMIS fluxgate magnetometer, in: The THEMIS Mission, pp. 235–264, Springer, http://link.springer.com/chapter/10.1007/978-0-387-89820-9_11, 2009.

Ciofi, C., Gianatti, R., Dattilo, V., and Neri, B.: Ultra Low Noise Current Sources, in: IEEE Instrumentation and Measurement Technology Conference, Ottawa, Canada, http://edge.rit.edu/edge/P10345/public/repo/Documentation/Comparable%20Products/UltraLowNoiseCurrentSources_Ciofi.pdf, 1997.

Costa, T., Piedade, M. S., and Santos, M.: An ultra-low noise current source for magnetoresistive biosensors biasing, in: 2012 IEEE Biomedical Circuits and Systems Conference (BioCAS), pp. 73–76, doi:10.1109/BioCAS.2012.6418507, http://ieeexplore.ieee.org/lpdocs/epic03/wrapper.htm?arnumber=6418507, 2012.

Egan, M.: The 20-bit DAC is the easiest part of a 1-ppm-accurate precision voltage source, Analog Dialogue, 44, http://www.analog.com/media/en/analog-dialogue/volume-44/number-2/articles/20-bit-dac-and-accurate-precision-voltage-source.pdf, 2010.

Fleddermann, R., Trobs, M., Steier, F., Heinzel, G., and Danzmann, K.: Intrinsic Noise and Temperature Coefficients of Selected Voltage References, IEEE Transactions on Instrumentation and Measurement, 58, 2002–2007, doi:10.1109/TIM.2008.2006133, http://ieeexplore.ieee.org/lpdocs/epic03/wrapper.htm?arnumber=4655612, 2009.

Halloin, H., Prat, P., and Brossard, J.: Long term characterisation of electronic components, http://www.phys.ufl.edu/lisasymposiumx/resources/contributions/posters/Halloin.pdf, 2014.

Harrison, L. T.: Current sources & voltage references, Embedded technology series, Newnes, Amsterdam, digitaler nachdr. edn., 2009.

Ioan, C., Tibu, M., and Chiriac, H.: Magnetic noise measurement for vacquier type fluxgate sensor with double excitation, Journal of optoelectronics and advanced materials, 6, 705–708, http://cat.inist.fr/?aModele=afficheN&cpsidt=16265880, 2004.

Koch, R. H. and Rozen, J. R.: Low-noise flux-gate magnetic-field sensors using ring- and rod-core geometries, Applied Physics Letters, 78, 1897–1899, doi:10.1063/1.1358852, http://aip.scitation.org/doi/abs/10.1063/1.1358852, 2001.

Koch, R. H., Deak, J. G., and Grinstein, G.: Fundamental limits to magnetic-field sensitivity of flux-gate magnetic-field sensors, Applied Physics Letters, 75, 3862–3864, doi:10.1063/1.125481, http://aip.scitation.org/doi/10.1063/1.125481, 1999.

Linear Technology Corp.: LTC6655 0.25ppm Noise, Low Drift Precision References. Rev. E., http://cds.linear.com/docs/en/datasheet/6655fe.pdf, 2014.

Linear Technology Corp.: LTZ1000/LTZ1000A Ultra Precision Reference. Rev. E., http://cds.linear.com/docs/en/datasheet/1000afe.pdf, 2015.

Merayo, J. M., Brauer, P., and Primdahl, F.: Triaxial fluxgate gradiometer of high stability and linearity, Sensors and Actuators A: Physical, 120, 71–77, doi:10.1016/j.sna.2004.11.014, http://linkinghub.elsevier.com/retrieve/pii/S0924424704008301, 2005.

Nielsen, O. V., Petersen, J. R., Primdahl, F., Brauer, P., Hernando, B., Fernandez, A., Merayo, J. M. G., and Ripka, P.: Development, construction and analysis of the'OErsted'fluxgate magnetometer, Measurement Science and Technology, 6, 1099, http://iopscience.iop.org/article/10.1088/0957-0233/6/8/004/meta, 1995.

Nosenko, V. K., Maslov, V. V., Kirilchuk, V. V., and Kochkubey, A. P.: Some industrial applications of amorphous and nanocrystalline alloys, Journal of Physics: Conference Series, 98, 072 016, doi:10.1088/1742-6596/98/7/072016, 2008.

Paperno, E.: Suppression of magnetic noise in the fundamental-mode orthogonal fluxgate, Sensors and Actuators A: Physical, 116, 405–409, doi:10.1016/j.sna.2004.05.011, http://www.sciencedirect.com/science/article/pii/S0924424704003498, 2004.

Rax, B. G., Lee, C. I., and Johnston, A. H.: Degradation of precision reference devices in space environments, IEEE Transactions on Nuclear Science, 44, 1939–1944, doi:10.1109/23.658965, 1997.

Sasada, I. and Kashima, H.: Simple design for orthogonal fluxgate magnetometer in fundamental mode, Journal of the Magnetics Society of Japan, 33, 43–45, https://www.jstage.jst.go.jp/article/msjmag/33/2/33_0901RF7129/_article/-char/ja/, 2009.

Scandurra, G., Cannatà, G., Giusi, G., and Ciofi, C.: Programmable, very low noise current source, Review of Scientific Instruments, 85, 125 109, doi:10.1063/1.4903355, http://scitation.aip.org/content/aip/journal/rsi/85/12/10.1063/1.4903355, 2014.

Texas Instruments Inc.: OPA2188 0.03-μV/°C Drift, Low-Noise, Rail-to-Rail Output, 36-V, Zero-Drift Operational Amplifiers, http://www.ti.com/lit/ds/symlink/opa2188.pdf, 2016.

Tsividis, Y. P.: Accurate analysis of temperature effects in I_C–V_{BE} characteristics with application to bandgap reference sources, Solid-State Circuits, IEEE Journal of, 15, 1076–1084, http://ieeexplore.ieee.org/xpls/abs_all.jsp?arnumber=1051519, 1980.

Turbitt, C., Matzka, J., Rasson, J., St-Louis, B., and Stewart, D.: An instrument performance and data quality standard for intermagnet one-second data exchange, in: Proceedings of the XVth IAGA Workshop on Geomagnetic Observatory Instruments and Data Processing, Cadiz, Spain, 4-14 June 2012, edited by Hejda, P., Chulliat, A., and Catalán, M., pp. 186–188, http://nora.nerc.ac.uk/507228/1/Turbitt_etal_IAGAworkshop_OneSecondDataExchange_2013.pdf, 2013.

Vetoshko, P., Valeiko, M., and Nikitin, P.: Epitaxial yttrium iron garnet film as an active medium of an even-harmonic magnetic field transducer, Sensors and Actuators A: Physical, 106, 270–273, doi:10.1016/S0924-4247(03)00182-1, http://linkinghub.elsevier.com/retrieve/pii/S0924424703001821, 2003.

Vishay Precision Group, Inc.: DSMZ (Z foil). Ultra High Precision Bulk Metal® Z-Foil Surface Mount Voltage Divider, TCR Tracking of <0.1 ppm/°C, PCR of ±5 ppm at Rated Power and Stability of ±0.005 % (50 ppm), http://www.vishaypg.com/docs/63121/dsmz.pdf, 2015.

Vishay Precision Group, Inc.: VSMP Series (0603, 0805, 1206, 1506, 2010, 2512) (Z Foil) Ultra High Precision Foil Wraparound Surface Mount Chip Resistor, http://www.vishaypg.com/docs/63060/VSMP.pdf, 2016.

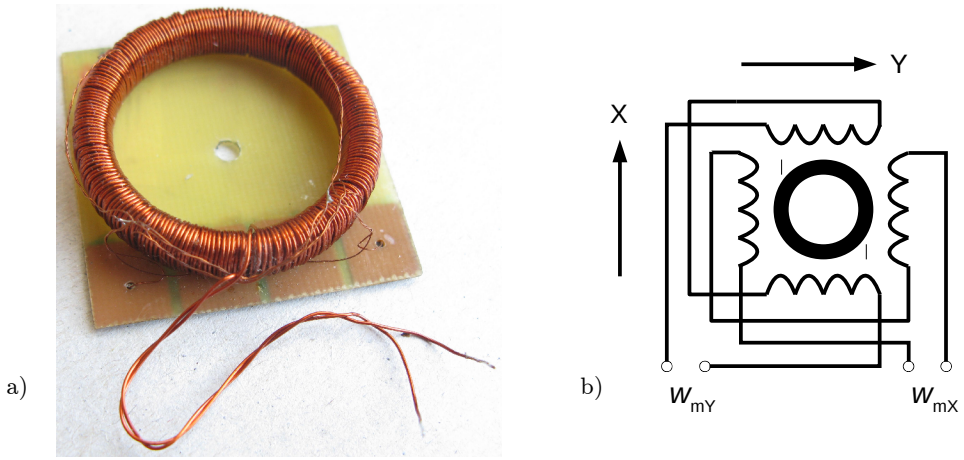

Figure 1. Fluxgate sensor FGS32/11: a) general view and b) measuring windings connection diagram.

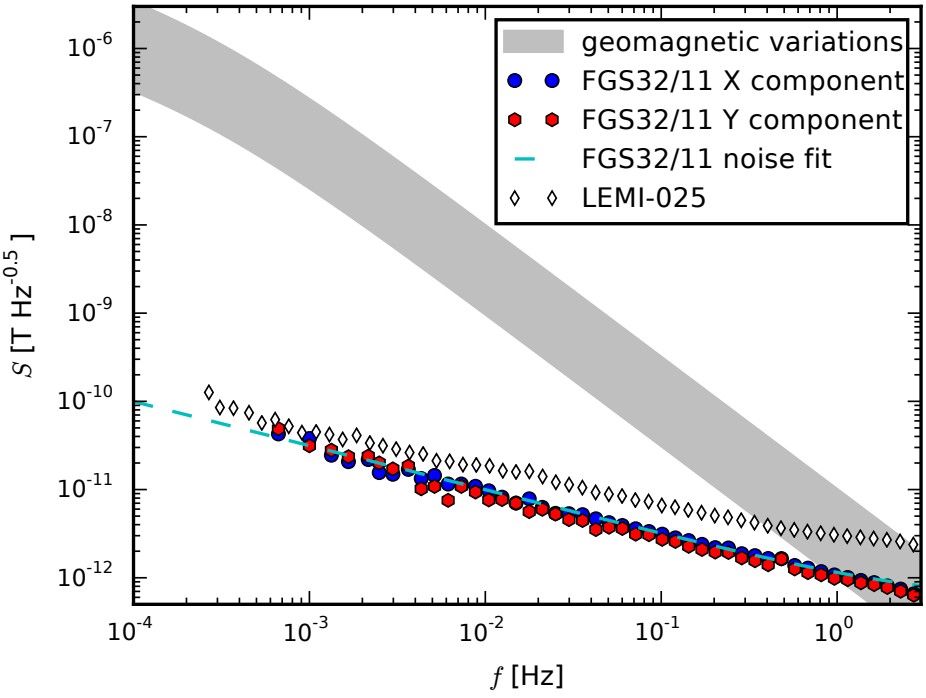

Figure 2. Noise spectra of flux-gate variometers.

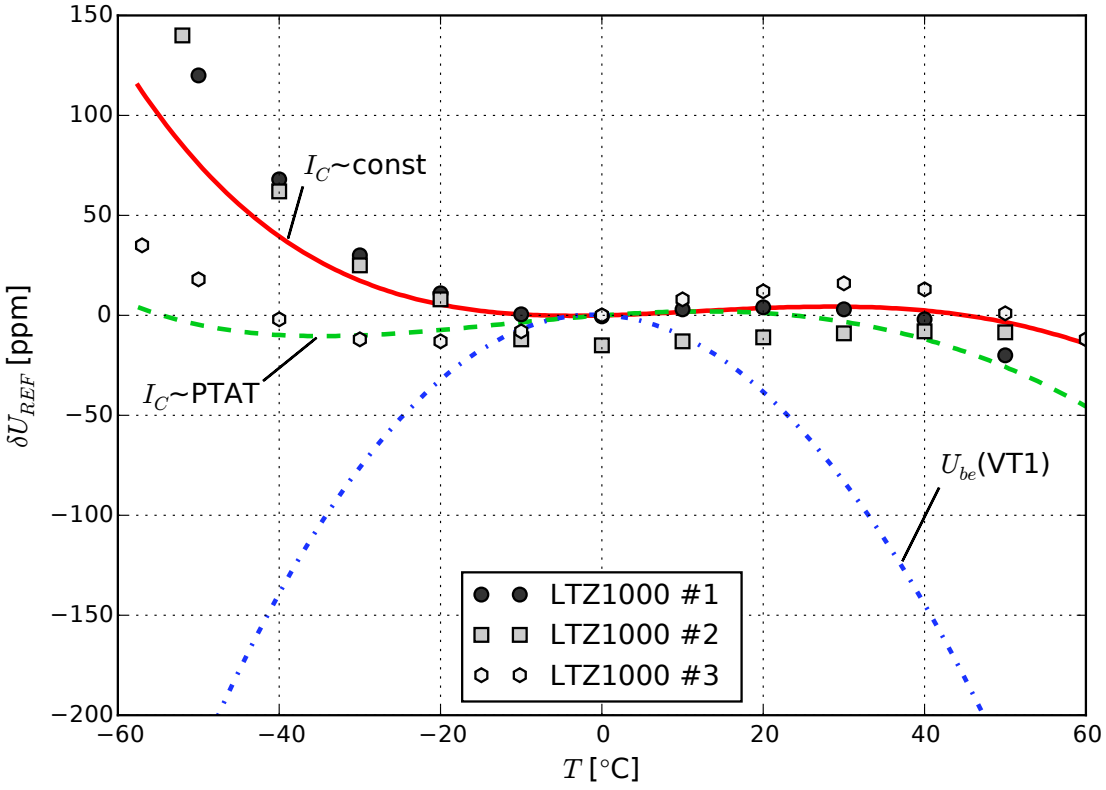

Figure 3. Temperature dependence of LTZ1000 reference voltage – simulated results (lines) and experimental data (marks).

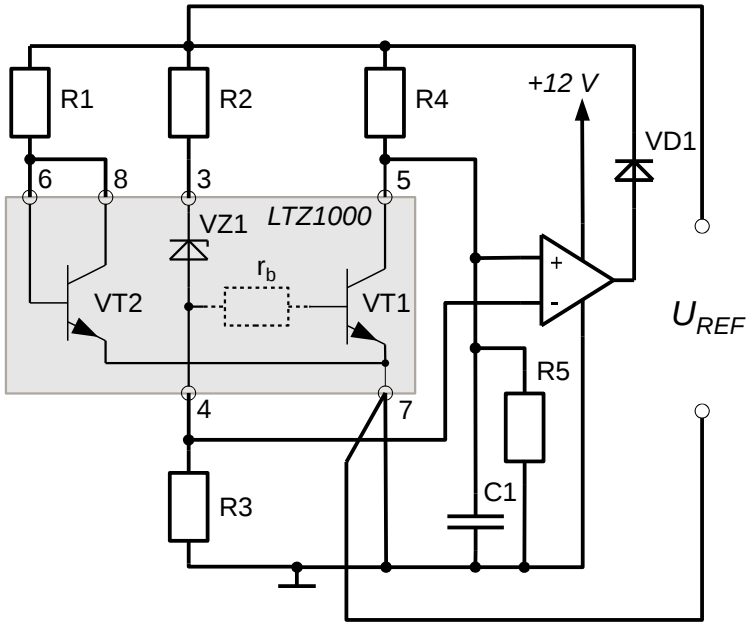

Figure 4. LTZ1000 configuration.

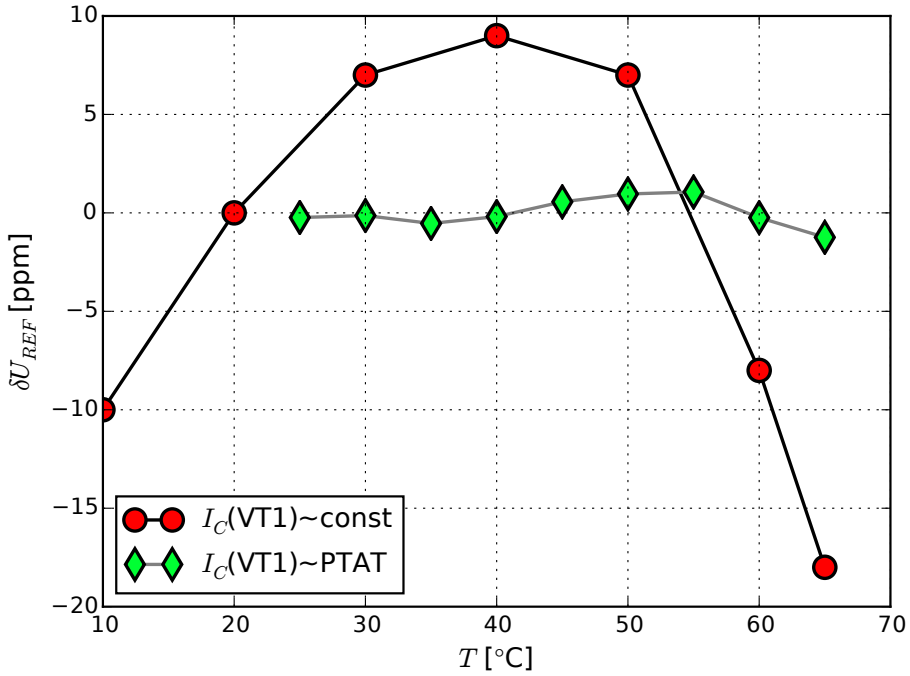

Figure 5. LTZ1000 voltage curvature correction.

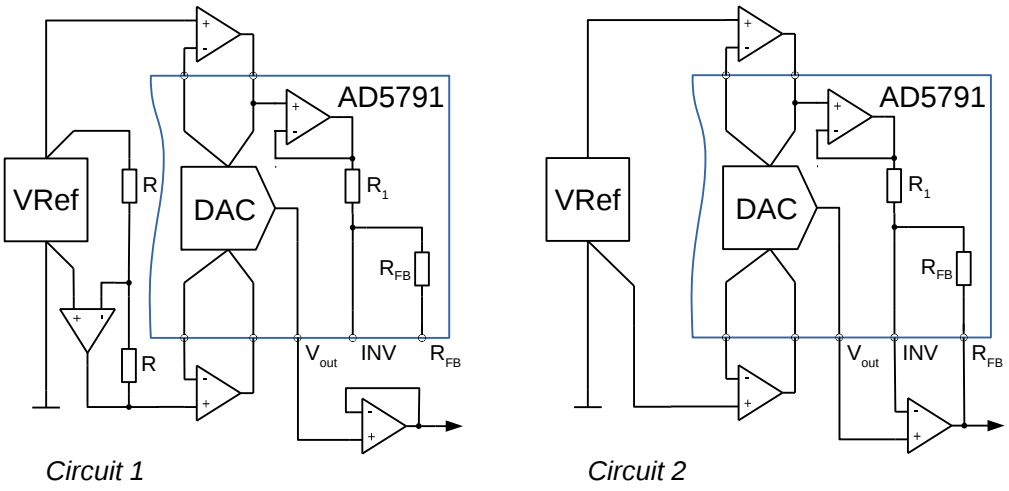

Figure 6. Digital to analog converter configurations.

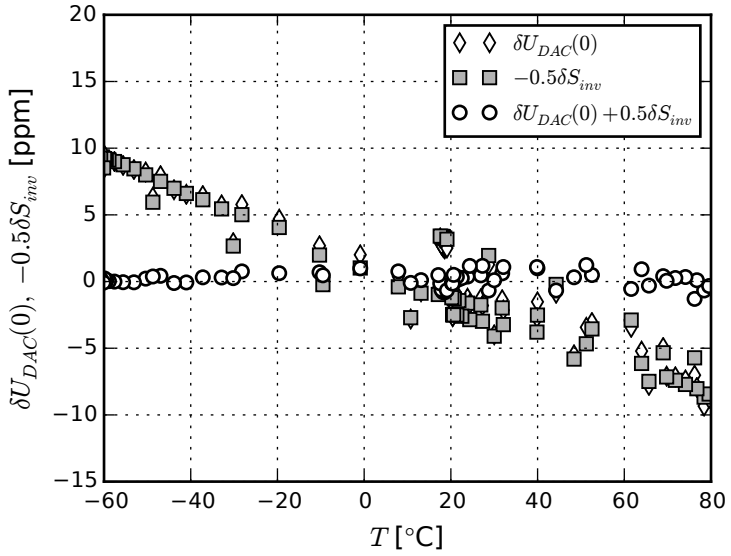

Figure 7. Temperature drift of the voltage reference inverter scale factor and the DAC zero offset.

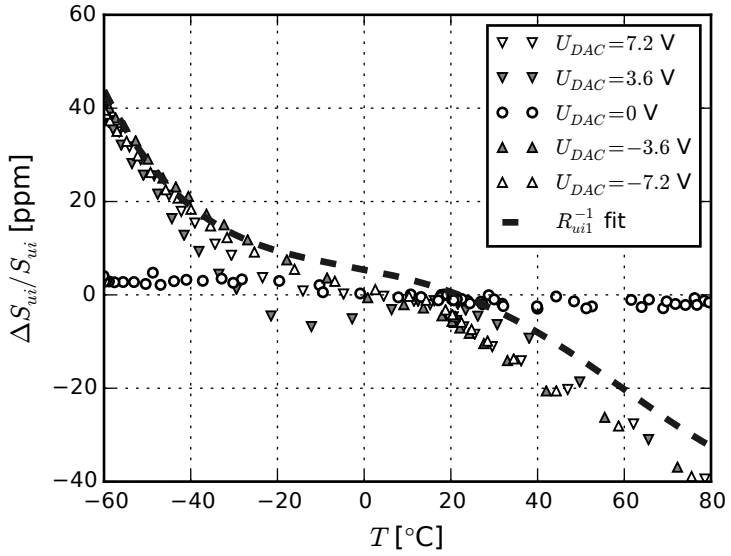

Figure 8. Temperature drift of the voltage-to-current converter transformation factor.

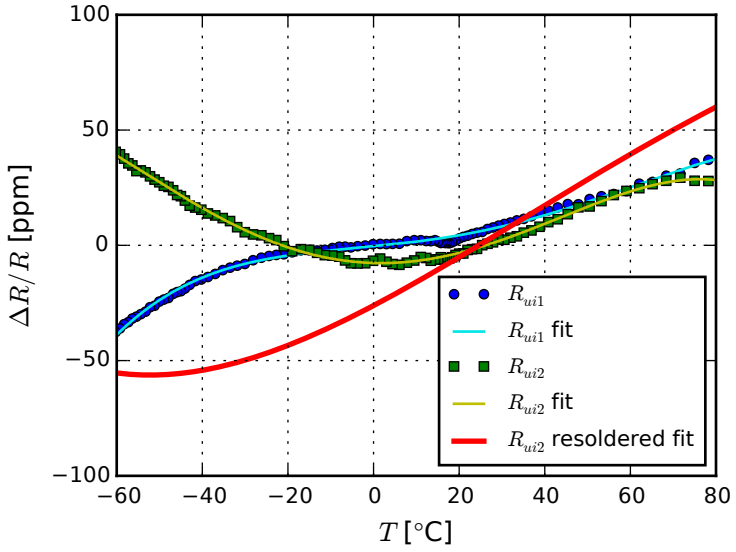

Figure 9. VSMP0805 resistors temperature dependences.

Table 1. Noise level of some digitally controlled current sources.

	Noise level (10^{-9} $Hz^{-0.5}$)		
Current source	0.01 Hz	0.1 Hz	1.0 Hz
Current source A (Ciofi et al., 1997)	7.5	1.4	0.27
Current source B (Scandurra et al., 2014)	no data	12	3
Current source C (Costa et al., 2012)	no data	no data	30
Requirements to the DCCS	71	22	7.1

Table 2. Noise level of some precision voltage references.

	Noise level (10^{-9} $Hz^{-0.5}$)		
Voltage reference	0.01 Hz	0.1 Hz	1.0 Hz
AD587LN (subsurface Zener) (Fleddermann et al., 2009)	250	70	19
LT1021BCN8-5 (subsurface Zener) (Fleddermann et al., 2009)	700	230	70
LT1236ACN8-5 (subsurface Zener) (Fleddermann et al., 2009)	600	130	35
~~LTZ1000 (subsurface Zener)~~ LTC6655-2.5 (bandgap) (Linear Technology Corp., 2014)	no data	~~33~~ 68	~~9~~ 28
~~LTC6655BHMs8-5 (bandgap)~~ LTZ1000 (subsurface Zener) (Linear Technology Corp., 2015)	~~2000~~ no data	~~1000~~ 33	~~700~~ 9
MAX6126 (proprietary) (Fleddermann et al., 2009)	230	100	50
MAX6250ACSA (subsurface Zener) (Fleddermann et al., 2009)	400	150	40
MAX6350 (subsurface Zener) (Halloin et al., 2014)	1000	600	100
VRE305 (subsurface Zener) (Halloin et al., 2014)	4000	2000	400

Table 3. Noise level of the digitally controlled current source

Frequency (Hz)	Noise level (10^{-9} Hz$^{-0.5}$)						Requirements
	$I_{out} = 0$		$I_{out} = I_{min}$		$I_{out} = I_{max}$		
	circuit 1	circuit 2	circuit 1	circuit 2	circuit 1	circuit 2	
1.0	4	**8**	**9**	**16**	**9**	**9**	$\leq$7.1
0.1	7	14	22	**39**	22	22	$\leq$22
0.01	15	42	70	**150**	70	70	$\leq$71